

Research Article

Tracing the origin of the placental trophoblast cells in mouse embryo development[†]

Shanshan Guo^{1,2,‡}, Xiuhong Cui^{1,‡}, Xiangxiang Jiang^{1,‡},
Shuguang Duo¹, Shiwen Li¹, Fei Gao^{1,2,*} and Hongmei Wang^{1,2,*}

¹State Key Laboratory of Stem Cell and Reproductive Biology, Institute of Zoology, Chinese Academy of Sciences, Beijing 100101, China and ²University of Chinese Academy of Sciences, Beijing, China

***Correspondence:** State Key Laboratory of Stem Cell and Reproductive Biology, Institute of Zoology, Chinese Academy of Sciences, Beijing 100101, China. Tel: 86-010-64807187; E-mail: wanghm@ioz.ac.cn (H. Wang); or Tel: 86-010-64807593; E-mail: gaof@ioz.ac.cn (F. Gao).

[†]**Grant Support:** The Ministry of Science and Technology of the People's Republic of China (2016YFC1000208 and 2017YFC1001401).

[‡]These authors contributed equally to this work.

Received 2 August 2019; Revised 3 September 2019; Editorial Decision 3 October 2019; Accepted 6 October 2019

Abstract

The placenta, which originates from the trophectoderm (TE), is the first organ to form during mammalian embryogenesis. Recent studies based on bioinformatics analysis have revealed that heterogeneous gene expression initiates cell-fate decisions and directs two distinct cell fates by modulating the balance of pluripotency and differentiation as early as the four-cell stage. However, direct developmental evidence to support this is still lacking. To address at which stage the cell fate of the TE and inner cell mass (ICM) is determined, in this study, we administered a microinjection of Cre mRNA into a single blastomere of the *mTmG* mouse at different cleavage stages before implantation to examine the distributions of the descendants of the single-labeled cell in the mouse fetus and the placenta at E12.5. We found that the descendants of the labeled cells at the two-cell stage contributed to both the placenta and the fetus. Notably, the derivatives of the labeled cells at the four-cell stage fell into three categories: (1) distributed in both embryonic and extraembryonic lineages, (2) distributed only in mouse placental trophoblast layers, or (3) distributed only in the lineage derived from the ICM. In addition, these results fell in line with single-cell studies focusing on gene expression patterns that characterize particular lineages within the blastocyst. In conclusion, this study shows that the four-cell blastomeres differ in their individual developmental properties insofar as they contribute to either or both the ICM and trophoblast fate.

Summary sentence

The four-cell blastomeres differ in their individual developmental properties insofar as they contribute to either or both the embryonic and extraembryonic lineage.

Key words: Cre mRNA, the *mTmG* mouse, placental trophoblast fate, the four-cell stage

Introduction

The formation of the zygote heralds the beginning of a new generation in mammals. After cleavage and compaction, the mouse blastocyst forms by E3.5 and organizes into three cell lineages: the

trophectoderm (TE), epiblast (EPI), and primitive endoderm (PE) when the blastocyst prepares for implantation [1–3]. As development proceeds, the TE will develop into the placenta; the EPI gives rise to the future fetus; and the PE forms the yolk sac. The mature

mouse placenta is composed of three principal layers: an outer layer of trophoblast giant cells [4, 5], a middle spongiotrophoblast layer, and the innermost labyrinth, which contains cells of both trophoblast and mesodermal origin that will develop into the fetal components of the placental vascular network [6, 7]. The placenta plays a large part in the exchange of materials between the maternal and fetal environments [8, 9], in addition to involvement in immune protection of the fetus [5]. As the main structural and functional components, the origin of the trophoblast lineage in the placenta remains an unresolved issue.

The lineage specification between the TE and the ICM is the earliest cell-fate determination during embryonic development [10, 11]. Many studies have been performed to trace cell lineages in the early mouse embryo with different approaches, such as optical lineage tracing [12–15] and sequence-based lineage tracing [16]. It was assumed that blastomeres at the two-cell stage are totipotent and were not biased in their contribution along the Em–Ab axis of the blastocyst [17–19]. This view, however, is challenged as the study shows that in separated two-cell stage blastomeres, only one generates the functional blastocyst with sufficient epiblast cells [20], and a current study discovered heterogeneities between sister blastomeres of late two-cell stage embryo [21]. In contrast to the controversy at two-cell stage embryos, a viewpoint, that heterogeneous gene expression initiates cell-fate decisions, as early as the four-cell stage, is now gaining support as recent studies have demonstrated heterogeneity in four-cell-stage embryos, which exhibits differences in gene expression [16, 22–24] and developmental potential [25, 26]. PRDM14 [24] and Sox21 [16] were asymmetrically distributed among four-cell-stage blastomeres, lower levels of which promote extraembryonic fate over pluripotency. These advances came from the studies performed in preimplantation or early postimplantation mouse embryos; however, two labeling experiments performed at the two-cell stage resulted in different cell distribution patterns at different developmental stages [27], which led to the present study examining the distribution of labeled cells at a later developmental stage.

In this study, *mTmG* mice [28] were used to trace the cell fate of blastomeres at different embryonic stages. The blastomeres were labeled with injection of Cre mRNA at the two-cell to eight-cell stage. We observed that the derivatives of the labeled blastomere at the four- and eight-stages display three types of distribution patterns between the fetus and placenta at E12.5, and an increased bias of labeled blastomeres is observed at the eight-cell stage. In addition, we applied single-cell RNA-seq on sorted green fluorescent protein (GFP)-positive cells from the blastocysts, expression analysis of genes implicated in TE vs. ICM lineage bias indicated that both the four- and eight-cell blastomeres displayed three-cell-fate potentials. This lineage tracing strategy provides new insights into cell-fate decisions and allows us to re-examine the distributions of descendants of the labeled blastomeres after implantation.

Materials and methods

Mice

Wild-type CD1 mice were purchased from Charles River Laboratories China Inc. and housed with an artificial 12:12 h light cycle (temperature, 22–24 °C; relative humidity, 40–50%). The laboratory of Haibin Wang presented the *mTmG* mice. All animal experiments were approved by the animal ethic committee and the Institutional Animal Care and Use Committee, Institute of Zoology, Chinese Academy of Sciences.

Embryo collection

For the lineage tracing experiments, 6-week-old wild-type CD1 females were superovulated by injection of 10 IU pregnant mare serum gonadotropin followed by 10 IU human chorionic gonadotropin after 46–48 h. The *mTmG* [28] male mice were crossed with the superovulated females. One-cell stage embryos were flushed from swollen ampullae with M2 medium (H3506, Sigma) containing 0.5 mg/ml of hyaluronidase (H3506, Sigma) several times to remove the surrounding cumulus cells. The embryos at the early two-, four- or eight-cell stages were obtained from the oviduct and then moved to drops of EmbryoMax potassium simplex optimized medium (KSOM) (MR-107-D, Specialty Media) covered with paraffin oil after washing several times in M2 medium and cultured in KSOM medium in an incubator at 37 °C and 5% CO₂.

Generation of Cre mRNA

The recombinant plasmid pXT7-CRE was constructed by Biomed, China. The pXT7-CRE construct was linearized with XbaI and then the linearized plasmid to be transcribed was examined on a gel to confirm that cleavage was complete. According to the instructions from the mMESSAGE mMACHINETM T7 Kit (AM1344, Invitrogen), the linearized plasmid was transcribed in vitro. Cre mRNA was purified with the RNeasy Mini Kit (D40724, QIAGEN) and diluted in ddH₂O at a final concentration of 0.2 µg/µl.

Cell labeling

To label a single blastomere, Cre mRNA was injected at the concentration of 0.2 µg/µl into the nucleus of one blastomere from one, two-, four- and eight-cell-stage embryos, and then morphologically normal embryos were transferred into oviducts of pseudopregnant CD1 female mice.

Immunofluorescence

The fetuses and placentas were collected at E12.5 and fixed with 4% paraformaldehyde overnight at 4 °C. The fixed fetuses and placentas were dehydrated through 70, 90, and 100% ethanol and then embedded in paraffin wax. Immunofluorescence was conducted on 6-µm sections. After dewaxing and rehydrating, the sections were blocked with 2% bovine serum albumin (BSA) in phosphate-buffered saline (PBS) for 1 h. The sections were then incubated overnight at 4 °C with primary antibodies (Supplementary Table S1). The slides were incubated with secondary antibodies for 1 h at room temperature. The nuclei were stained with 6'-diamidino-2-phenylindole (DAPI). The sections were washed with PBS (3 × 5 min) between each step. Images were obtained with a Zeiss 780 confocal microscope and processed with ZEN software.

Statistical analysis

The data were analyzed by χ^2 -tests using the RStudio. *P* values of less than 0.05 were considered significant.

Isolation of individual blastomeres at the blastocyst stage

The injected embryos were cultured in KSOM medium until the blastocyst stage. Then the blastocysts were exposed to acid Tyrode solution to remove the zona pellucida and washed thoroughly in PBS with 0.1% BSA. The denuded embryos were treated with 0.5% trypsin for 10 min at 37 °C and dispersed them using thorough pipetting. Single GFP-positive cells were deposited into 2.5 µl lysis buffer

with a mouth pipette, which were subsequently reverse transcribed and amplified using the modified smart-seq2 method [29].

Reads mapping and gene expression quantification

The Smart-seq2 data with paired-end reads were processed were processed using the standard pipeline of Drop-seq_tools-2.0.0 [30] (<http://mccarrolllab.com/dropseq/>). For read2, bases 1–8 were tagged with the cell barcode, and bases 9–16 were tagged with molecule barcode. Read1 was trimmed at the 5' end to remove adaptor and template switch oligo (TSO) sequence, and the 3' end was trimmed to remove poly(A) sequences with length 6 or more. We used STAR aligner to align the filtered fastq file to *Mus_musculus*. GRCm38.84 genome reference files were incorporated with enhanced green fluorescent protein (EGFP) annotation information. The gene expression matrix (count value) for each cell was generated with the Digital Expression command. The gene number of single cells from mouse blastocysts is shown in the Supplementary Data. The raw data and processed expression matrix data were deposited in the Gene Expression Omnibus database (accession number: GSE133639, the access token will be provided upon request).

Analysis of single-cell RNA-seq data

We used Seurat V3.0 R package to analyze the single-cell data. First, we used the *vst* and *mean*. *Var*. plot methods individually to calculate variable genes of 579 cells with at least 1000 genes expressed and performed unsupervised clustering. After excluding ambiguous ICM or TE cells, we obtained 525 cells for the following analysis. The t-distributed stochastic neighbor embedding (t-SNE) plot of 525 cells, unsupervised clustering, and generation of a heat map showing differentially expressed genes were performed with the Seurat package. We defined EGFP-positive cells by the scaled value of the EGFP gene, which was more than 2, and 116 EGFP-positive cells were obtained. Only EGFP-positive cells with more than 2 were further used for the statistical analysis, and the results are shown in the pie chart.

Results

GFP signals were efficiently activated by Cre mRNA injection

To study the cell-fate determination of different blastomeres, a single blastomere from mTmG transgenic mice was injected with Cre mRNA at different embryonic stages. The distribution of descendants of labeled blastomeres was examined at E12.5. In this mouse model, green fluorescence will be activated after Cre excision (Figure 1). To verify this system, Cre mRNA was injected at the one-cell stage and the distribution of GFP-positive cells was examined at E12.5. As shown in Figure 2, both fetuses and placentas were GFP-positive under whole-mount observation. To examine the detailed distribution of the GFP-positive cells, immunofluorescence was performed with serial paraffin sections. The cells in the fetus and placenta were uniformly GFP positive (Figure 2D–G). To strengthen the data on embryos and placentas that are indeed green, even if the low-magnification overview images appear black, PCR across the LoxP recombination site excluded the presence of GFP-negative cells (Figure 2C and Supplementary Figure S3), indicating GFP was efficiently activated by Cre mRNA injection during the embryonic stage.

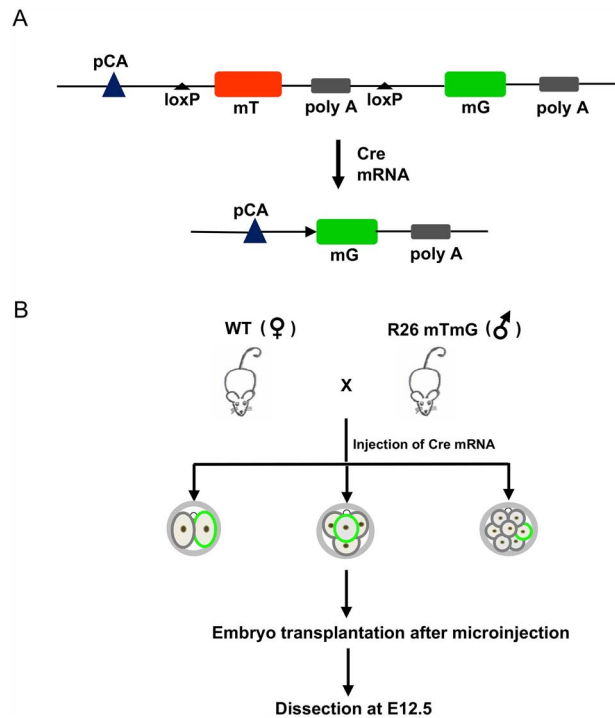


Figure 1. Schematic diagram for labeling single blastomeres. (A) The *mT/mG* construct before and after Cre-mediated recombination. (B) Working model for labeling a single blastomere at the two-cell, four-cell, or eight-cell stages by microinjection of Cre mRNA.

Progeny of blastomeres at the two-cell stage distributed in both the fetus and placenta

To investigate whether the cell fate of each blastomere is determined in a two-cell-stage embryo, a single blastomere of a two-cell embryo was randomly injected with Cre mRNA. The fetuses and placentas were collected at E12.5. As shown in Figure 3, GFP signals were detected in both fetuses and placentas in 27 of the collected embryos. In other embryos, a GFP signal was not detected in either the fetus or placenta. The GFP signal was not activated in these embryos, which is probably due to the low efficiency of Cre activity. The results of immunostaining experiments showed that GFP-positive cells were randomly distributed along body axes and in all layers of the placenta (Figure 3B and C). These results suggest that the blastomeres at the two-cell stage display equal developmental potential and that the cell fate of different blastomeres is not determined at this stage.

The developmental bias of blastomeres was noted at the four-cell stage

Next, the developmental potential of blastomeres at the four-cell stage was examined by single blastomere Cre mRNA injection. A total of 94 morphologically normal fetuses and placentas were examined at E12.5. Three different distribution patterns of GFP-positive cells were observed. The whole-mount images and the representative images of immunostaining were shown in Figure 4. In 19 embryos, the GFP signal was only detected in the placenta and the GFP signal was completely absent in fetal tissue (Figure 4A–C). The results of immunostaining with serial sections also showed that GFP-positive cells were distributed randomly in all layers of the placenta, but no positive cells were observed in the fetal tissues.

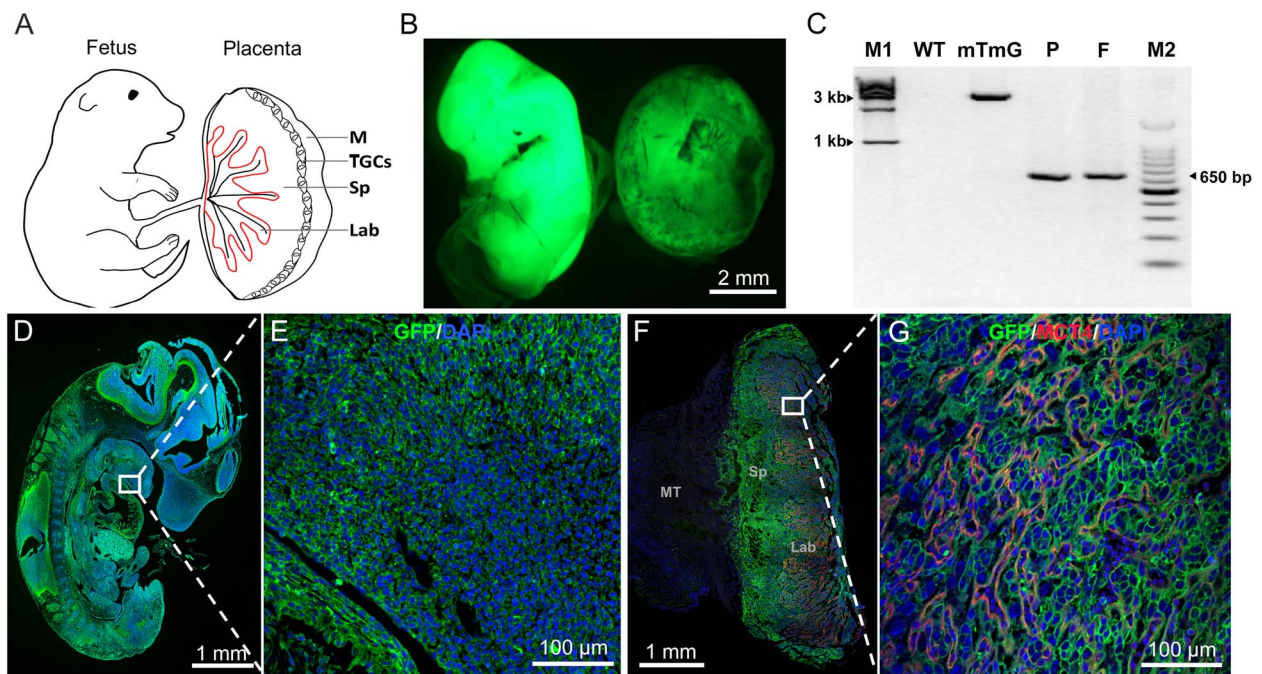


Figure 2. GFP-positive cells were detected in both the fetus and placenta when Cre mRNA was injected at the one-cell stage. (A) Schematic representation of the constitutions of embryo and placenta or trophoblast. (B) Whole mount image of GFP-positive fetus and placenta at E12.5. (C) The PCR products encompassing the LoxP sites amplified from the genomic DNA prepared from WT, mTmG, P and F. M1, Marker 1 (1 kb); WT, wild-type; mTmG, tail of the mTmG mouse without Cre recombination; P, E12.5 placenta with Cre recombination; F, E12.5 fetus with Cre recombination; M2, Marker 2 (100 kb). (D) A representative section of the E12.5 fetus showing that GFP-positive cells are distributed along the fetal body axes (F) A representative section of the E12.5 placenta showing that GFP-positive cells are distributed in all layers and that the maternal decidua is GFP negative. (E and G) Higher magnifications show the GFP-positive cells in the fetus and placenta. MCT4 and DAPI were used to label the labyrinth layer of the placenta and the nuclei, respectively. MT, maternal decidua; Sp, spongiotrophoblast layer; Lab, labyrinth layer.

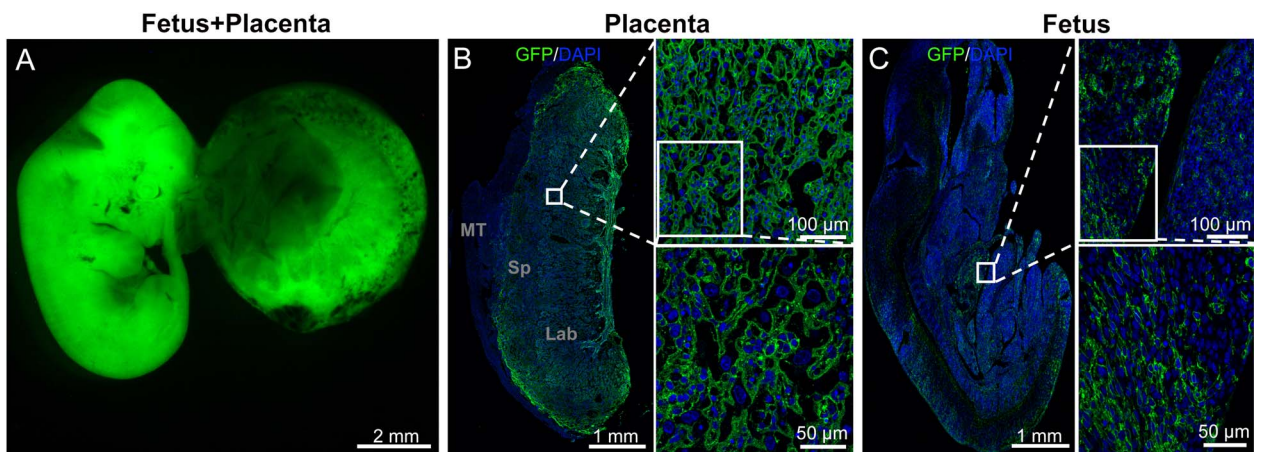


Figure 3. Descendants of a labeled single blastomere at the two-cell stage were randomly distributed in the placenta and fetal tissues at E12.5. (A) Whole mount image of GFP-positive fetus and placenta at E12.5. (B) GFP-positive cells were distributed in all layers of the placenta at E12.5. (C) A representative section of the E12.5 fetus showing that GFP-labeled cells are randomly distributed in the fetus. Nuclei were labeled with DAPI. MT, maternal decidua; Sp, spongiotrophoblast layer; Lab, labyrinth layer.

By contrast, in 18 embryos (Figure 4D–F), the GFP signals were detected only in the fetal tissue, and no GFP-positive cells were detected in the placenta. In 57 embryos, GFP signals were detected in both the placenta and fetus (Figure 4G–L), which was similar to the distribution pattern observed at the two-cell stage. Interestingly, in 15 out of the 57 embryos, a GFP signal was detected in both the fetus and placenta by whole-mount observation. However, to further

verify the origin of these cells, the immunostaining results of placenta sections showed that the localization of GFP-positive cells was colocalized with Laminin-positive cells (Figure 4K), and Laminin was used to label vascular endothelial cells of the placenta [9]. Because the fetal vessels in the placenta are derived from the ICM, these embryos were considered fetus positive and placenta negative. These results suggest that different developmental potentials of signal blastomeres

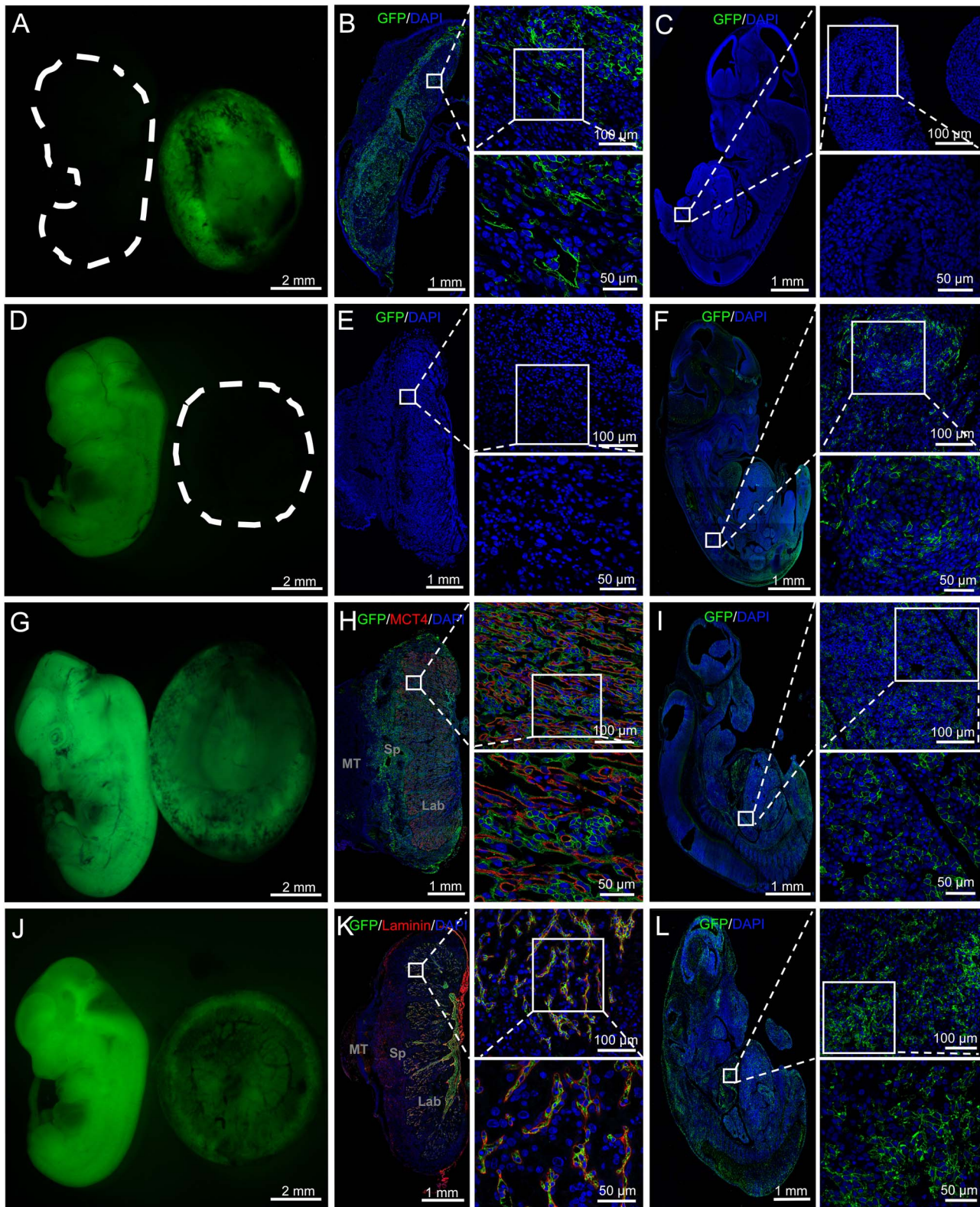


Figure 4. Three different distribution patterns of GFP-positive cells when a single blastomere was labeled at four-cell stage. (A, D, G and J) Whole mount image of GFP-positive fetus and placenta at E12.5; (B and E) sections of the placentas in A and D, respectively; (C and F) sections of the fetuses in A and D, respectively. (H and I) A representative section showing that GFP-positive cells are distributed randomly in the placenta and fetus. (K) A representative section showing GFP-positive cells are only detected in the fetus vessels of the placenta. (L) GFP-positive cells are intermingled with GFP-negative cells in the fetus. MCT4 and DAPI were used to, respectively, label the labyrinth layer of the placenta and the nuclei. MT, maternal decidua; Sp, the spongiotrophoblast layer; Lab, the labyrinth layer.

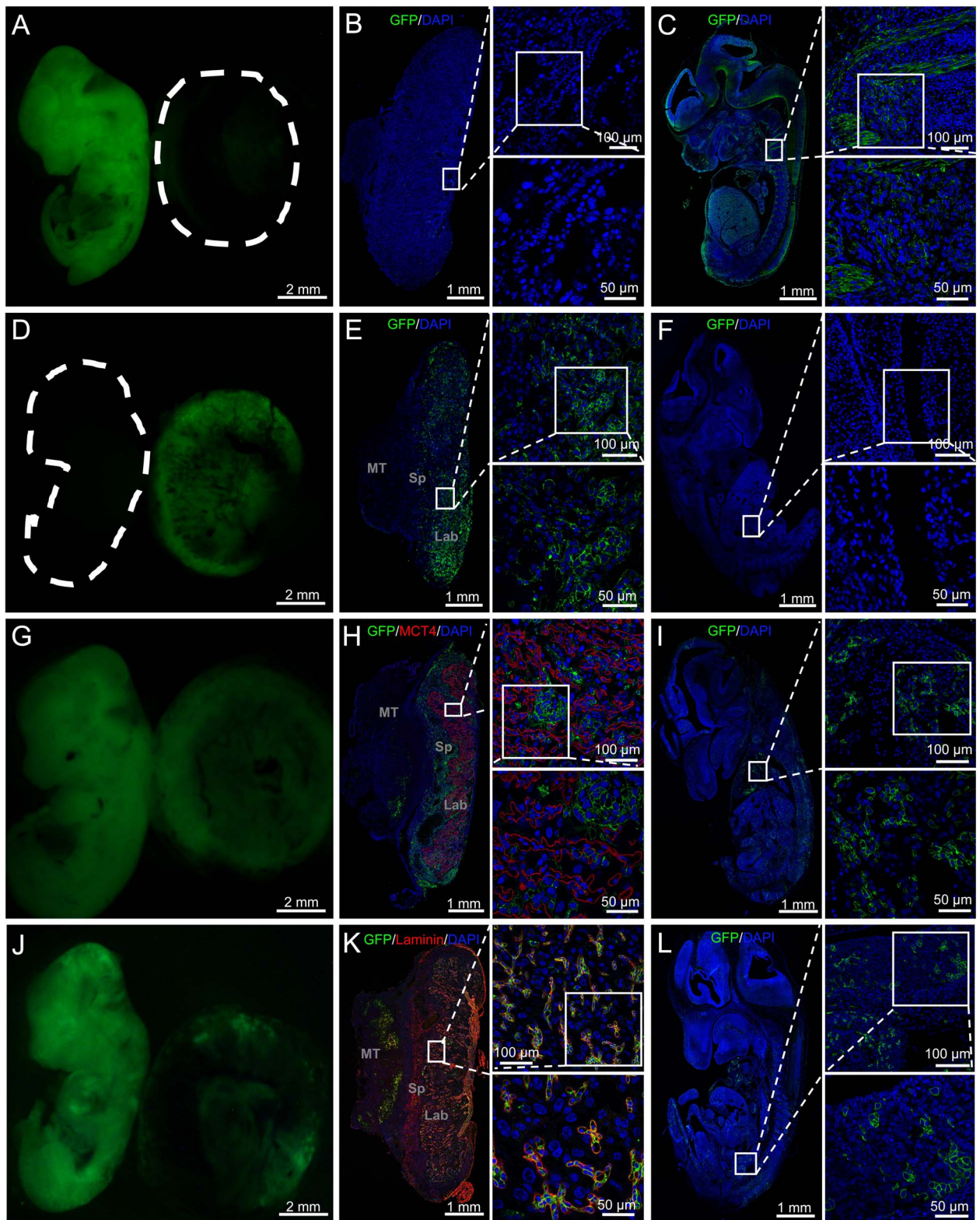


Figure 5. The distribution of the descendants labeled a single blastomere at eight-cell stage. (A, D, G, and J) Whole mount image of GFP-positive fetus and placenta at E12.5; (B and E) sections of the placentas in A and D, respectively; (C and F) sections of the fetuses in A and D, respectively. (H and I) A representative section showing that GFP-positive cells are distributed randomly in the placenta and fetus. (K) A representative section showing GFP-positive cells are detected in the fetal blood vessels of the placenta. (L) GFP-positive cells are intermingled with negative cells in the fetus. Laminin was used to label fetal vessels of the placenta. MCT4 and DAPI were used to label the labyrinth layer of the placenta and the nuclei, respectively. MT, maternal decidua; Sp, spongiotrophoblast layer; Lab, labyrinth layer.

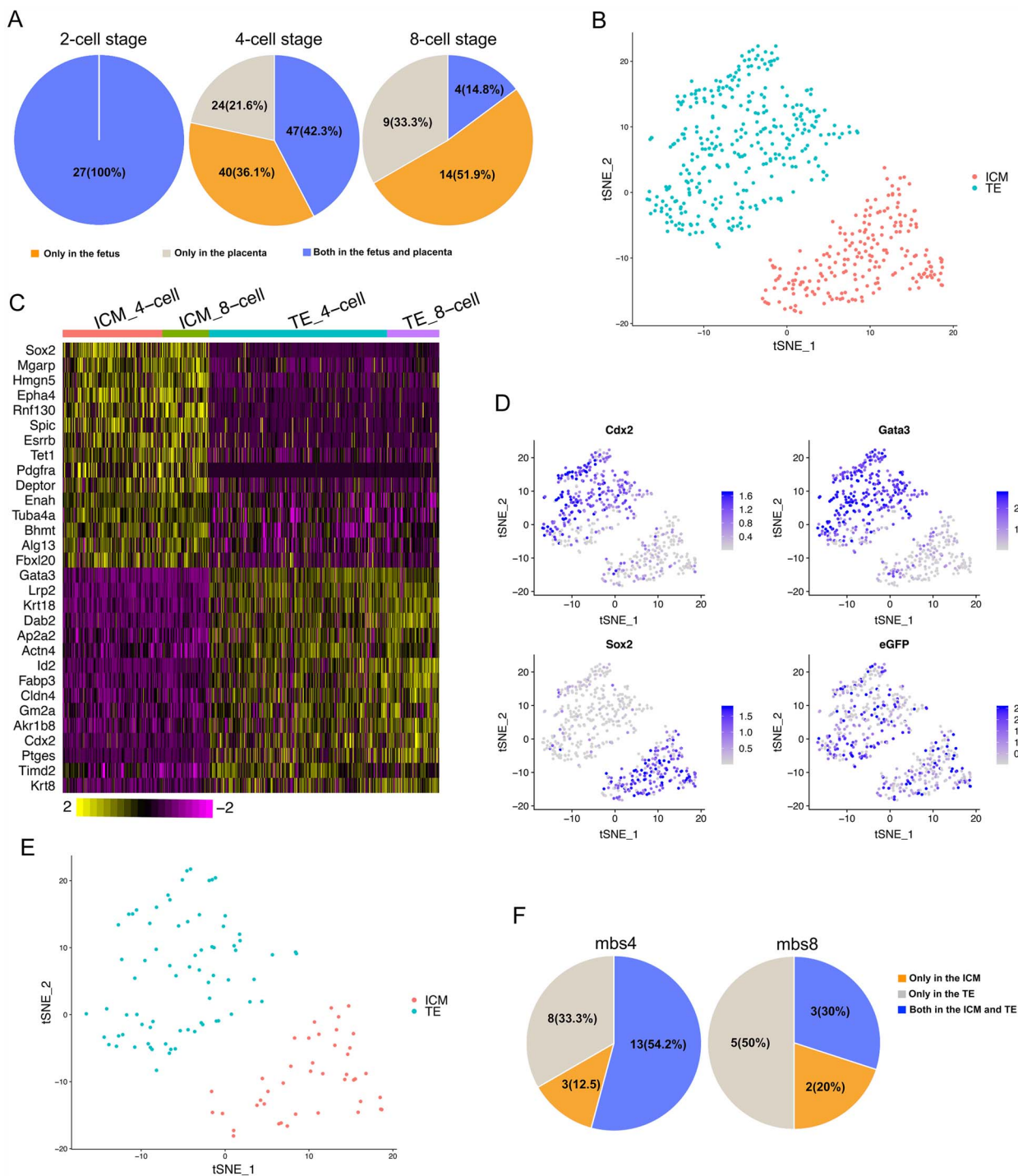


Figure 6. The TE and ICM lineage segregation of labeled cells in the blastocysts. (A) Summary of distribution patterns of the labeled cells in the mouse placenta and fetus at E12.5. (B) t-SNE plot showing unsupervised clustering of 525 blastocyst cells (ICM and TE). (C) Heat map illustrating the differential expression of genes that are implicated in TE vs. ICM lineage bias. (D) t-SNE plot showing the expression of Cdx2, Gata3 and Sox2 in TE and ICM cells. (E) The t-SNE plot shows the defined GFP-positive cells selected from the samples shown in Figure 6B. (F) A pie chart depicting the distribution patterns of the GFP-positive cells in the blastocyst. mbs4, labeling at the four-cell stage; mbs8, labeling at the eight-cell stage.

start to establish at the four-cell stage. Some blastomeres develop into fetus and some blastomeres prior to develop into placenta. However, the cell fate of all the blastomeres is not determined at this stage, and approximately 50% of them displayed unbiased developmental potential.

To determine whether the contribution of the progeny labeled at the four-cell stage toward different trophoblast cell types varies, we examined the sections of E12.5 GFP-positive placenta to determine the distribution of labeled progeny in the different trophoblast layers, including syncytiotrophoblast, trophoblast giant cells, and

spongiotrophoblast (Supplementary Figure S1). However, we did not find a clearly skewed distribution of the labeled progeny to individual placental trophoblast layers. This indicates that the four-cell blastomeres show no clear developmental predisposition to follow individual placental trophoblast cell fates.

The majority of blastomeres at the eight-cell stage displayed bias in developmental potential

The developmental potential of single blastomeres at the eight-cell stage was also examined by Cre mRNA injection. A total of 17 morphologically normal fetuses and placentas were obtained at E12.5. Consistent with the embryos at the four-cell stage, three types of GFP-positive cells were observed at this stage (Figure 5). However, the ratio of embryos with fetus and placenta double-positive signal was significantly reduced compared to that at the four-cell stage. Most of them were either fetus positive or placenta positive. As shown in Figure 5K, GFP-positive cells were also observed in fetal blood vessels of the placenta in three embryos. In addition, the labeled progeny was observed in all trophoblast layers (Supplementary Figure S2). These results suggest that the cell fate of most blastomeres has been determined at the eight-cell stage, the eight-cell blastomeres show no clear bias of developmental potential toward individual trophoblast cell types.

Analysis of the four- and eight-cell blastomeres on developmental potential with single-cell RNA-seq

We observed three distribution patterns of the labeled cells in the mouse placenta and fetus at E12.5 when the Cre injection was performed at the four- or eight-cell stage (Figure 6A). Comparison of the data from the Cre injection at the four- and eight-cell stage indicated that the eight-cell blastomeres showed a greater tendency ($\chi^2 P < 0.05$) to contribute to either the embryonic part or abembryonic part.

To validate the expression patterns of some key genes that are implicated in TE vs. ICM lineage bias, we isolated labeled cells at the blastocyst stage and performed at least candidate-based gene expression analyses. A total of 597 single cells were collected from 51 blastocysts. After filtering out the low-quality cells (see Materials and methods), 525 cells were selected for further analysis (Supplementary Table S2 and Supplementary Figure S4). We first identified ICM and TE populations with unsupervised clustering (Figure 6B). As presented in Figure 6C, the transcriptomes of individual cells in the ICM and TE populations were significantly different. TE marker genes (caudal-type homeobox transcription factor-2, *Cdx2*; Gata binding protein-3, *Gata3*) and the ICM marker gene (octamer-binding transcription factor-4, *Oct4*) were highly expressed in TE and ICM populations, respectively (Figure 6D). We filtered EGFP-positive cells by the scaled value of the EGFP gene, which was more than 2. A total of 116 EGFP-positive cells from 44 blastocysts were obtained (Figure 6E), of which 34 blastocysts (mbs4, $n = 24$; mbs8, $n = 10$) with EGFP-positive cells ($n > 1$) were further analyzed (Supplementary Table S2). Expression analysis of candidate-based genes that are implicated in TE vs. ICM lineage bias indicated that both the four- and eight-cell blastomeres displayed three cell fate potentials (Figure 6F), which is consistent with our results of lineage tracing study in vivo.

Discussion

The cell fate of different blastomeres is established during cleavage after fertilization. However, the timing and exact regulatory mecha-

nism of cell-fate determination in mammals is still unclear because of the inherent developmental flexibility of the embryo. The cell-fate determination of blastomeres has been investigated previously using Cre-LoxP recombination technology [27]. In that study, a single blastomere was labeled at different embryonic stages with injection with Cre plasmid and distribution of progeny of blastomere at E8.5. They found that when the single blastomere was labeled at the four-cell stage, three types of distribution patterns were noted. By contrast, when the single blastomere was labeled at two-cell stage, the progeny of labeled blastomeres was ubiquitously contributed to both TE and ICM derivatives. This study raised a possibility that blastomeres exhibit three different cell fates at the four-cell stage. Interestingly, a recent report demonstrated that the blastomeres at the four-cell stage displayed two types of developmental potential [16]. The blastomere with lower levels of Sox21 contributed mostly to the TE lineage, whereas the rest of the blastomeres contributed to both TE and ICM. In accordance with the results of Fujimori et al. [27], the results of our study also showed that the two-cell blastomeres displayed unsupervised potential to both the ICM and TE derivatives, and the first cell fate choice of early blastomeres, toward ICM or trophoblast fate, has become determined at the four-cell stage. In consistent with the results in vivo, with single-cell RNA-seq on sorted GFP-positive cells from the blastocysts, expression analysis of genes implicated in TE vs. ICM lineage bias indicated that both the four- and eight-cell blastomeres displayed three cell-fate potentials. Based on the quantitative results at the four-cell stage, we speculate that the cell fate of two blastomeres was already established at this stage. One blastomere contributes to placenta, which is consistent with previous studies [16, 23, 27], whereas another blastomere contributes to the ICM derivatives. We also found that the number of blastomeres with developmental bias was significantly increased at the eight-cell stage compared to that of the four-cell stage. However, a small portion of blastomeres still contributed to both placenta and fetus. These results suggest that not all the blastomeres were cell fate determined at the eight-cell stage.

Taken together, our study demonstrated that the developmental bias of single blastomeres has been established at the four-cell stage and that blastomere with developmental potential to both TE and ICM derivatives were detected at this stage. The developmental bias was significantly increased at the eight-cell stage, but the cell fate of a small portion of undetermined blastomere also exist at this stage. The results of this study provide valuable information for better understanding of the spatiotemporal pattern of cell-fate determination during embryonic development.

Supplementary data

Supplementary data are available at *BIOLRE* online.

Acknowledgements

We sincerely appreciate Dr. Haibin Wang (Xiamen University, China) for providing the *mTmG* mice. We are most grateful to Dr. Wei Li (Institute of Zoology, Chinese Academy of Sciences) for helpful suggestions.

Authors' contributions

HW and FG conceived and designed the study. SG and XC performed the experiments. XJ was in charge of the bioinformatics analysis. SD offered technical assistance in microinjection. SL offered technical support in confocal

photography. SG drafted the original draft. FG, HW, and SG reviewed and edited the manuscript.

Conflict of interest

The authors have declared that no conflict of interest exists.

References

- Cross JC. Placental function in development and disease. *Reprod Fertil Dev* 2006; **18**:71–76.
- Kelly SJ. Studies of the developmental potential of 4- and 8-cell stage mouse blastomeres. *J Exp Zool* 1977; **200**:365–376.
- Plusa B, Piliszek A, Frankenberg S, Artus J, Hadjantonakis AK. Distinct sequential cell behaviours direct primitive endoderm formation in the mouse blastocyst. *Development* 2008; **135**:3081–3091.
- Simmons DG, Fortier AL, Cross JC. Diverse subtypes and developmental origins of trophoblast giant cells in the mouse placenta. *Dev Biol* 2007; **304**:567–578.
- Hu D, Cross JC. Development and function of trophoblast giant cells in the rodent placenta. *Int J Dev Biol* 2010; **54**:341–354.
- JRajC C. Placental development: lessons from mouse mutants. *Nature* 2001; **2**:338–348.
- Lee Adamson S, YL K, Whiteley J. Interactions between trophoblast cells and the maternal and fetal circulation in the mouse placenta. *Dev Biol* 2002; **250**:358–373.
- Cross JC, MH YL, Nozaki T, Whiteley K, Masutani M, Adamson SL. Trophoblast functions, angiogenesis and remodeling of the maternal vasculature in the placenta. *Mol Cell Endocrinol* 2002; **187**:207–212.
- Watson ED, Cross JC. Development of structures and transport functions in the mouse placenta. *Physiology (Bethesda)* 2005; **20**:180–193.
- Zernicka-Goetz M, Morris SA, Bruce AW. Making a firm decision: multifaceted regulation of cell fate in the early mouse embryo. *Nat Rev Genet* 2009; **10**:467–477.
- Graham SJ, Zernicka-Goetz M. The acquisition of cell fate in mouse development. How do cells first become heterogeneous? *Curr Top Dev Biol* 2016; **117**:671–695.
- Wilson I. I., Bolton E., Cuttler R. H.. Preimplantation differentiation in the mouse egg as revealed by microinjection of vital markers. *J Embryol Exp Morphol* 1972; **27**:467–479.
- Balakier H, Pedersen RA. Allocation of cells to inner cell mass and trophoblast lineages in preimplantation mouse embryos. *Dev Biol* 1982; **90**:352–362.
- Gardner L. The early blastocyst is bilaterally symmetrical and its axis of symmetry is aligned with the animal-vegetal axis of the zygote in the mouse. *Development* 1997; **124**:289–301.
- Zernicka-Goetz M, Pines J, Hunter S. M., Dixon J. P. C., Siemering K. R., Haseloff J., Evans M. Following cell fate in the living mouse embryo[J]. *Development* 1997; **124**: 1133–1137.
- Goolam M, Scialdone A, Graham SJL, Macaulay IC, Jedrusik A, Hupalowska A, Voet T, Marioni JC, Zernicka-Goetz M. Heterogeneity in Oct4 and Sox2 targets biases cell fate in 4-cell mouse embryos. *Cell* 2016; **165**:61–74.
- Alarcon VB, Marikawa Y. Deviation of the blastocyst axis from the first cleavage plane does not affect the quality of mouse postimplantation development. *Biol Reprod* 2003; **69**:1208–1212.
- Chrosicka A, Komorowski S, Maleszewski M. Both blastomeres of the mouse 2-cell embryo contribute to the embryonic portion of the blastocyst. *Mol Reprod Dev* 2004; **68**:308–312.
- Nami Motosugi TB, Polanski Z, Solter D, Hiragi T. Polarity of the mouse embryo is established at blastocyst and is not prepatterned. *Genes Dev* 2005; **19**:1081–1092.
- Casser E, Israel S, Witten A, Schulte K, Schlatt S, Nordhoff V, Boian M. Totipotency segregates between the sister blastomeres of two-cell stage mouse embryos. *Sci Rep* 2017; **7**:8299.
- Jiaqiang Wang LW, Feng G, Wang Y, Li Y, Li X, Liu C, Jiao G, Huang C, Shi J, Zhou T, Chen Q, Liu Z, et al. Asymmetric expression of LincGET biases cell fate in 2-cell mouse embryos. *Cell* 2018; **175**: 1887–1901.
- Torres-Padilla ME, Parfitt DE, Kouzarides T, Zernicka-Goetz M. Histone arginine methylation regulates pluripotency in the early mouse embryo. *Nature* 2007; **445**:214–218.
- Plachta N, Bollenbach T, Pease S, Fraser SE, Pantazis P. Oct4 kinetics predict cell lineage patterning in the early mammalian embryo. *Nat Cell Biol* 2011; **13**:117–123.
- Burton A, Muller J, Tu S, Padilla-Longoria P, Guccione E, Torres-Padilla ME. Single-cell profiling of epigenetic modifiers identifies PRDM14 as an inducer of cell fate in the mammalian embryo. *Cell Rep* 2013; **5**: 687–701.
- Tabansky I, Lenarcic A, Draft RW, Loulier K, Keskin DB, Rosains J, Rivera-Feliciano J, Lichtman JW, Livet J, Stern JN, Sanes JR, Eggan K. Developmental bias in cleavage-stage mouse blastomeres. *Curr Biol* 2013; **23**:21–31.
- Piotrowska-Nitsche K, Perea-Gomez A, Haraguchi S, Zernicka-Goetz M. Four-cell stage mouse blastomeres have different developmental properties. *Development* 2005; **132**:479–490.
- Fujimori T, Kurotaki Y, Miyazaki J, Nabeshima Y. Analysis of cell lineage in two- and four-cell mouse embryos. *Development* 2003; **130**:5113–5122.
- Muzumdar MD, Tasic B, Miyamichi K, Li L, Luo L. A global double-fluorescent Cre reporter mouse. *Genesis* 2007; **45**:593–605.
- Liu Y, Fan X, Wang R, Lu X, Dang Y-L, Wang H, Lin H-Y, Zhu C, Ge H, Cross JC, Wang H. Single-cell RNA-seq reveals the diversity of trophoblast subtypes and patterns of differentiation in the human placenta. *Cell Res* 2018; **28**:819–832.
- Macosko EZ, Basu A, Satija R, Nemes J, Shekhar K, Goldman M, Tirosh I, Bialas AR, Kamitaki N, Martersteck EM, Trombetta JJ, Weitz DA, et al. Highly parallel genome-wide expression profiling of individual cells using Nanoliter droplets. *Cell* 2015; **161**:1202–1214.